Supplementary Information (SI) for Journal of Materials Chemistry B.
This journal is © The Royal Society of Chemistry 2025

This SI replaces the original version
published on 11 Jun 2024

In Vitro and In Vivo Biocompatibility Assessment of Chalcogenide Thermoelectrics as Implants

Mingyuan Gao[1,#], Yiping Luo[2,3,#], Wen Li[1,*] Longpo Zheng[2,3*] and Yanzhong Pei[1,*]
[1]Interdisciplinary Materials Research Center, School of Materials Science and Engineering, Tongji Univ., 4800 Caoan Rd., Shanghai, 201804, China
[2]Center for Orthopaedic Science and Translational Medicine, Department of Orthopedics, Shanghai Tenth People's Hospital, School of Medicine, Tongji Univ., 301 Yanchang Rd., Shanghai 200072, China.
[3]Orthopedic Intelligent Minimally Invasive Diagnosis and Treatment Center, Shanghai Tenth People's Hospital, School of Medicine, Tongji Univ., 301 Yanchang Rd.,Shanghai 200072, China.
[#]The authors equally contributed
*Email: liwen@tongji.edu.cn (WL), dr.zheng@tongji.edu.cn (LZ), yanzhong@tongji.edu.cn (YP)

Table S1. Synthesis parameter for various thermoelectric materials

Material	Melting temperature/°C	Melting time/h	Annealing temperature/°C	Annealing time/d	Hot pressing temperature/°C	Hot pressing pressure/MPa	Hot pressing time/min
SnSe	950	12	500	2d	510	50	30
Ag_2Se	1050	8	500	2d	350	50	30
Cu_2Se	1150	12	800	3d	450	65	30
Bi_2Se_3	800	10	500	2d	500	80	20
Te	550	8	400	3d	400	90	20
GeTe	950	7	627	3d	600	80	50
SnTe	950	6	677	2d	627	60	30
MnTe	950	6	650	3d	600	65	30
Bi_2Te_3	800	10	500	2d	450	80	30
$Bi_2Te_{2.88}Se_{0.12}$	800	10	500	2d	420	80	30
$Bi_{0.5}Sb_{1.5}Te_3$	800	10	500	2d	400	50	30
Sb_2Te_3	723	6	400	2d	500	50	30

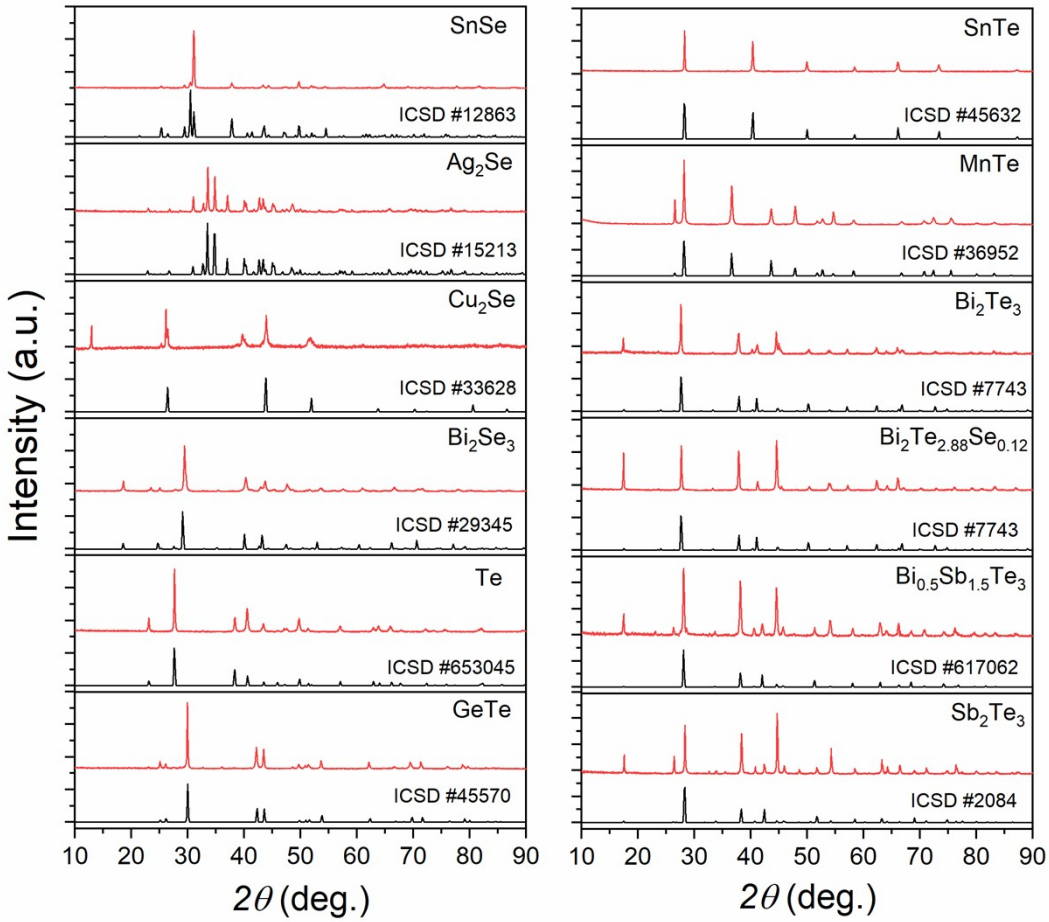

Fig. S1. Powder XRD patterns for various thermoelectric materials.

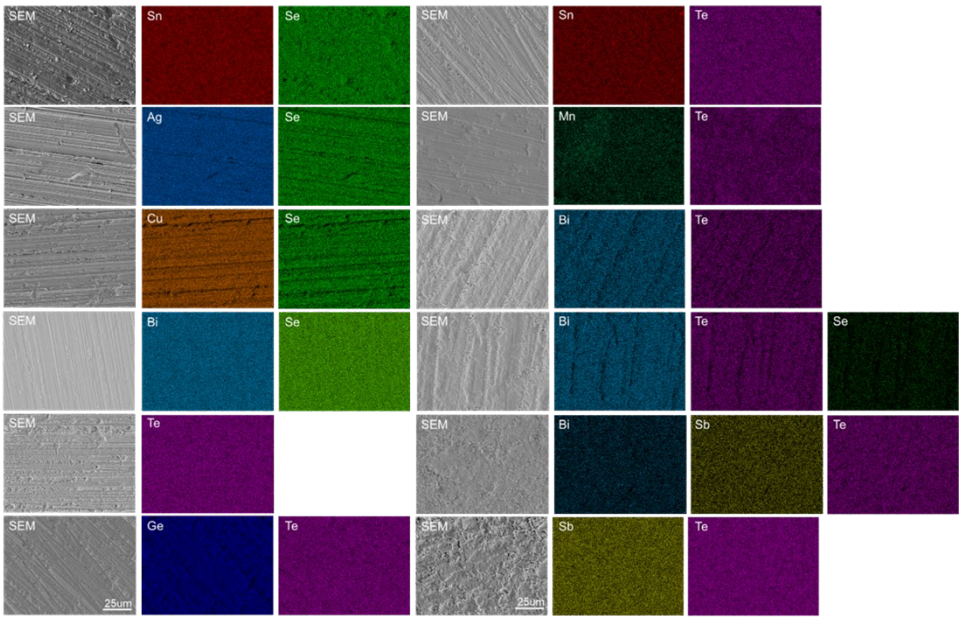

Fig. S2. SEM images and corresponding EDS mappings for various thermoelectric materials.

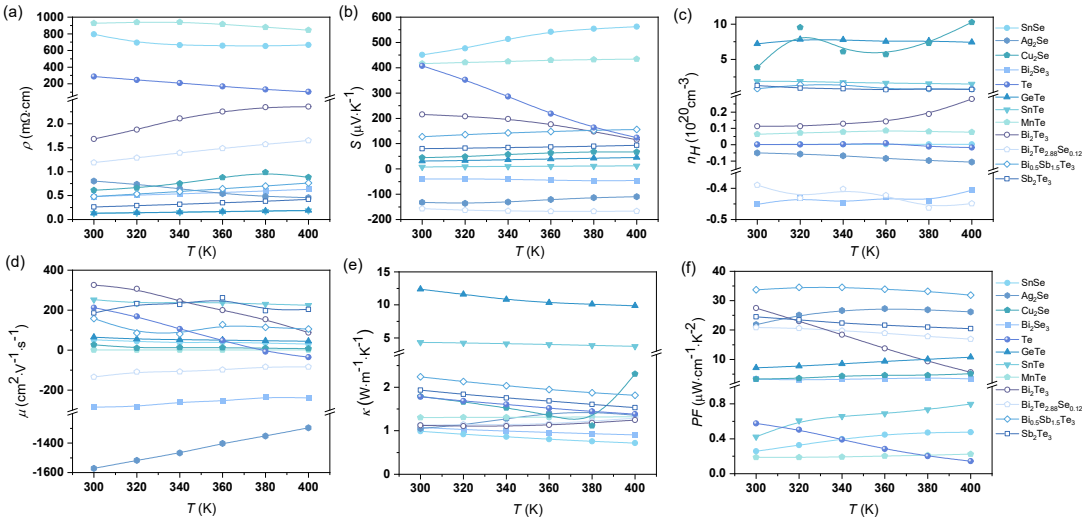

Fig. S3. Temperature dependent transport properties of resistivity (a), Seebeck coefficient (b), Hall carrier concentration (c), Hall carrier mobility (d), thermal conductivity (e) and power factor (f) for various thermoelectric materials.

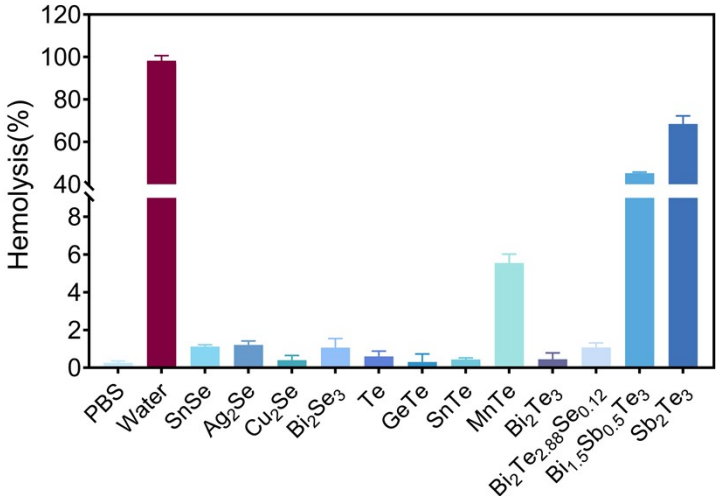

Fig. S4. Hemolytic effect of thermoelectric materials extracts after 2 h incubation with RBCs at 37 °C. Data are presented as the mean ± s.d. (n = 3 independent experiments)

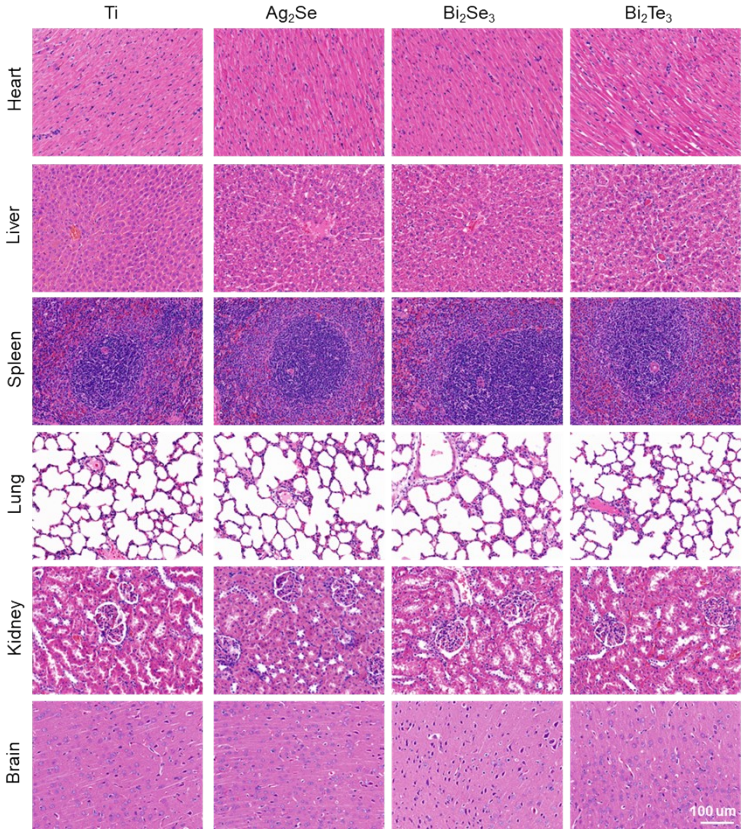

Fig.S5 Representative histological images stained with H&E of heart, liver, spleen, lung, spleen, kidney and brain organs after implantation of thermoelectric materials for 3 days (n = 3). The size of scale bar corresponds to 100 μm.

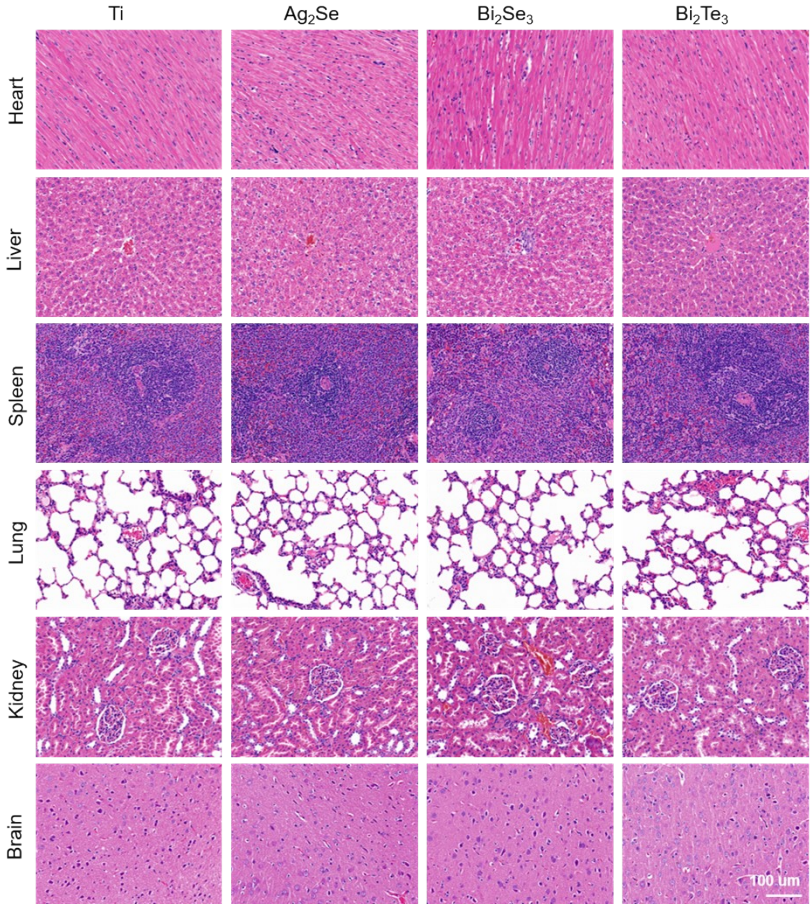

Fig. S6. Representative histological images stained with H&E of heart, liver, spleen, lung, spleen, kidney and brain organs after implantation of thermoelectric materials for 7 days (n = 3). The size of scale bar corresponds to 100 μm.

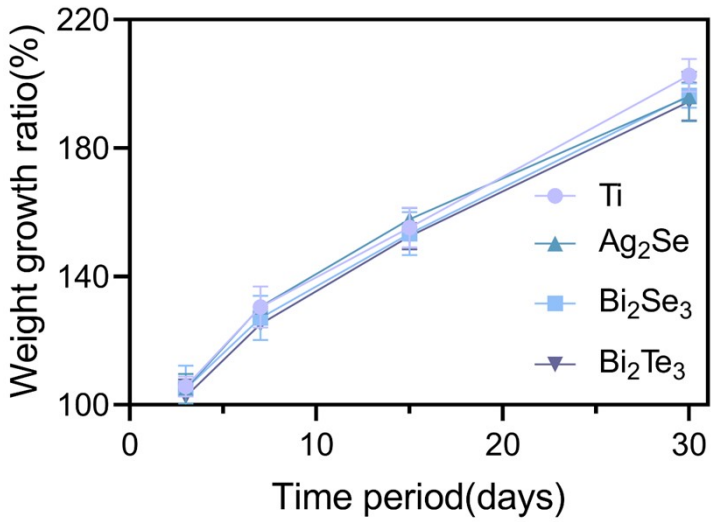

Fig. S7. Body weight tracking after the thermoelectric materials implanted subcutaneously in rats.

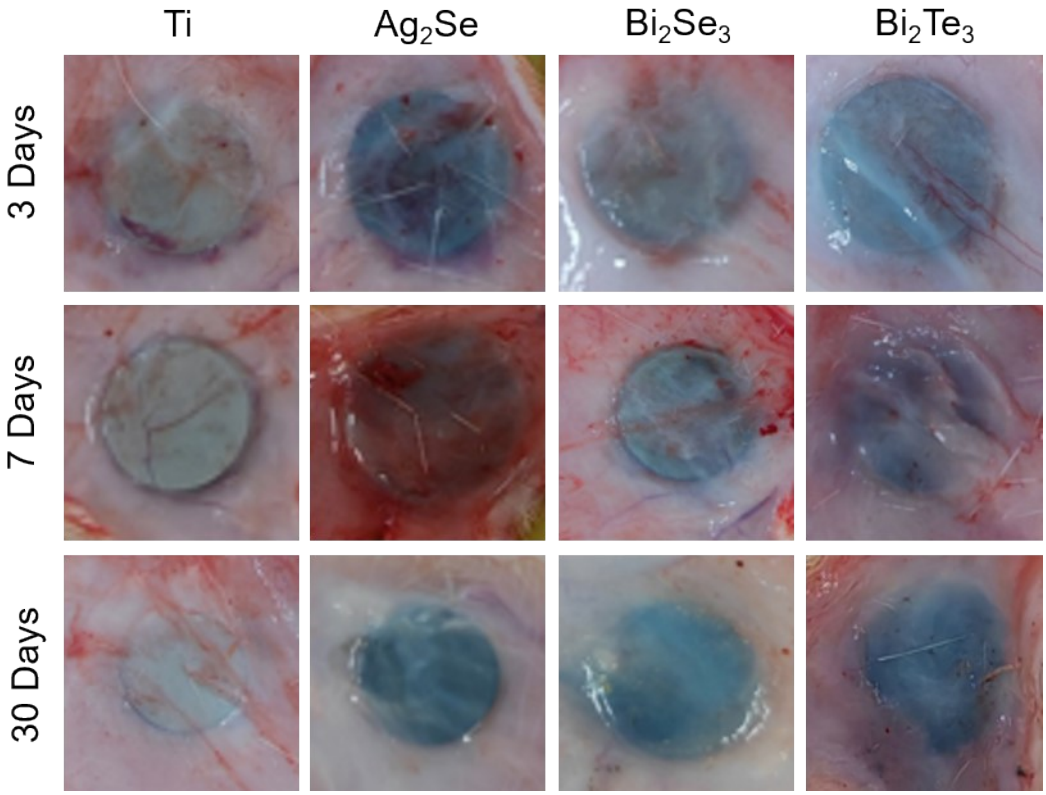

Fig. S8. General observation of Ti alloys and thermoelectric materials after subcutaneous implantation for 3, 7, and 30 days.

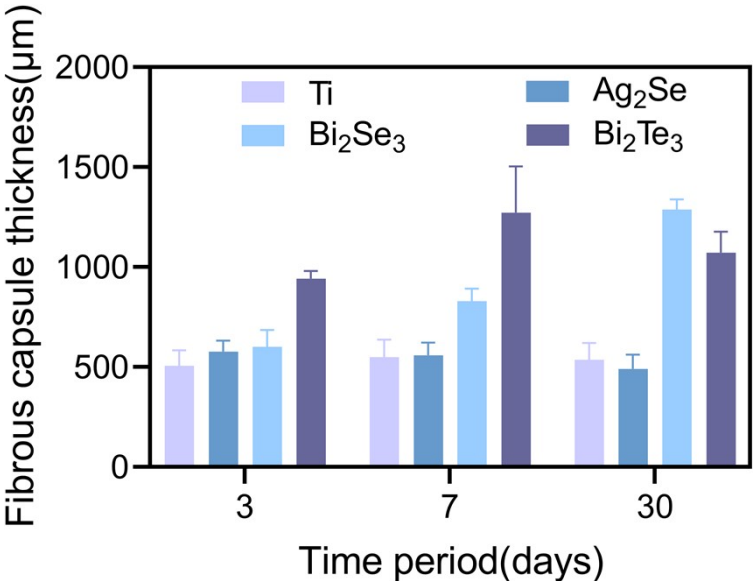

Fig.S9. Fibrous capsule thickness of Ti alloys and thermoelectric materials implanted subcutaneously in rats.

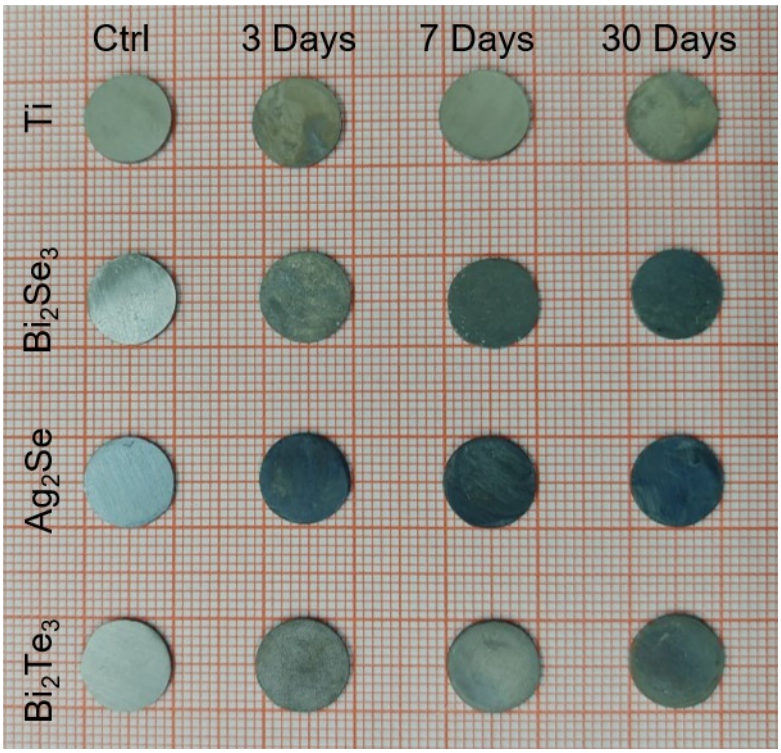

Fig. S10. Photos of Ti alloys and thermoelectric materials after subcutaneous implantation for 3, 7, and 30 days.

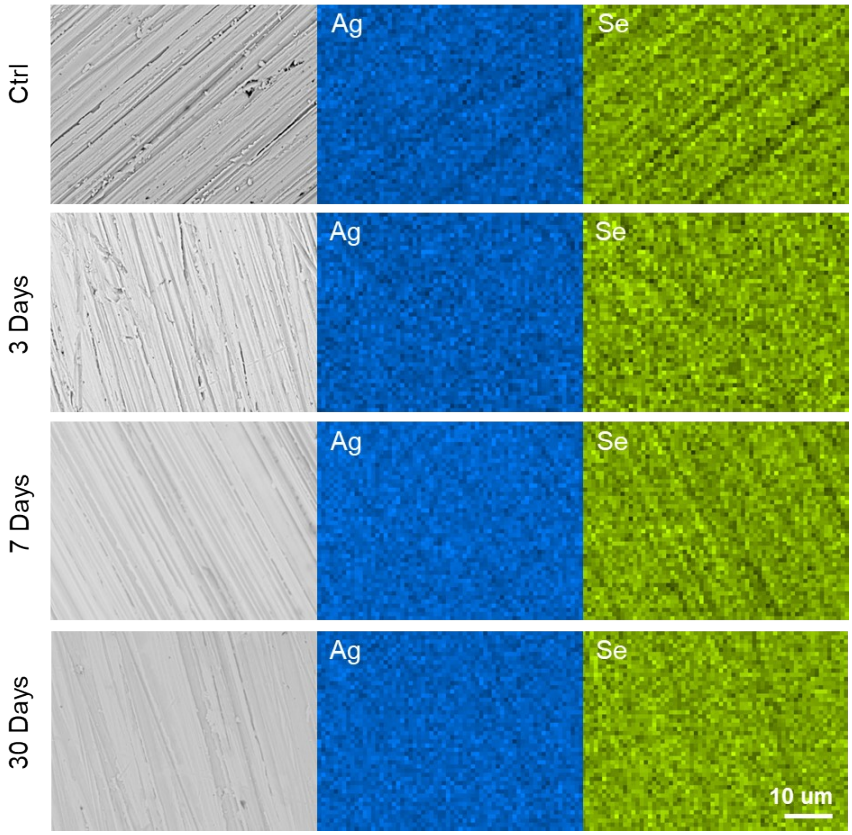

Fig. S11. SEM images and corresponding EDS mappings for Ag_2Se after subcutaneous implantation for 3, 7, and 30 days.

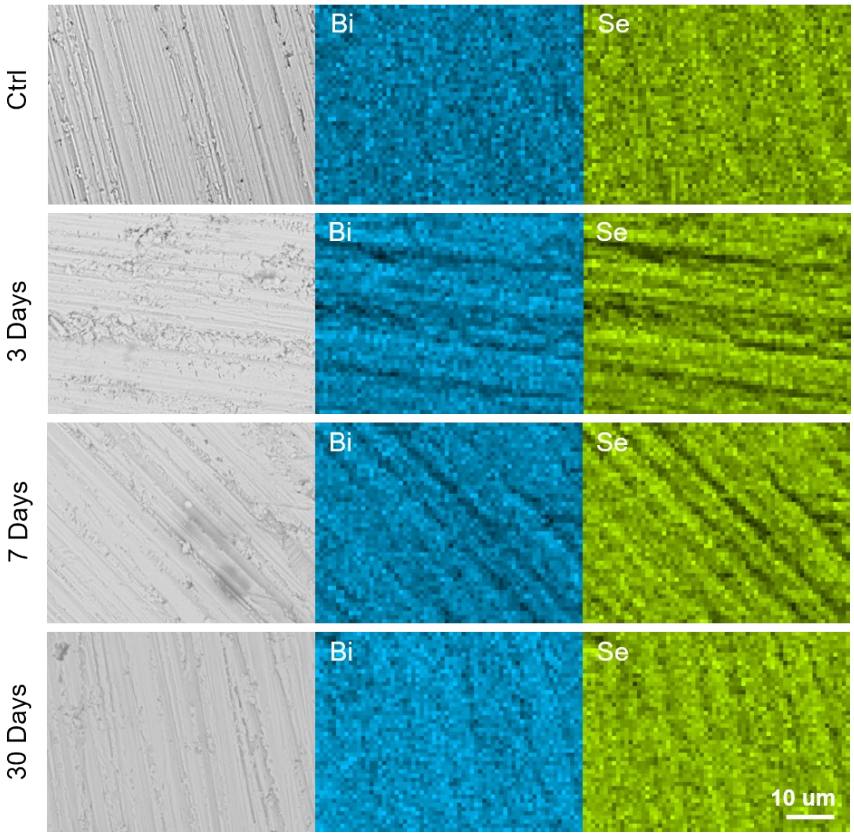

Fig. S12. SEM images and corresponding EDS mappings for Bi_2Se_3 after subcutaneous implantation for 3, 7, and 30 days.

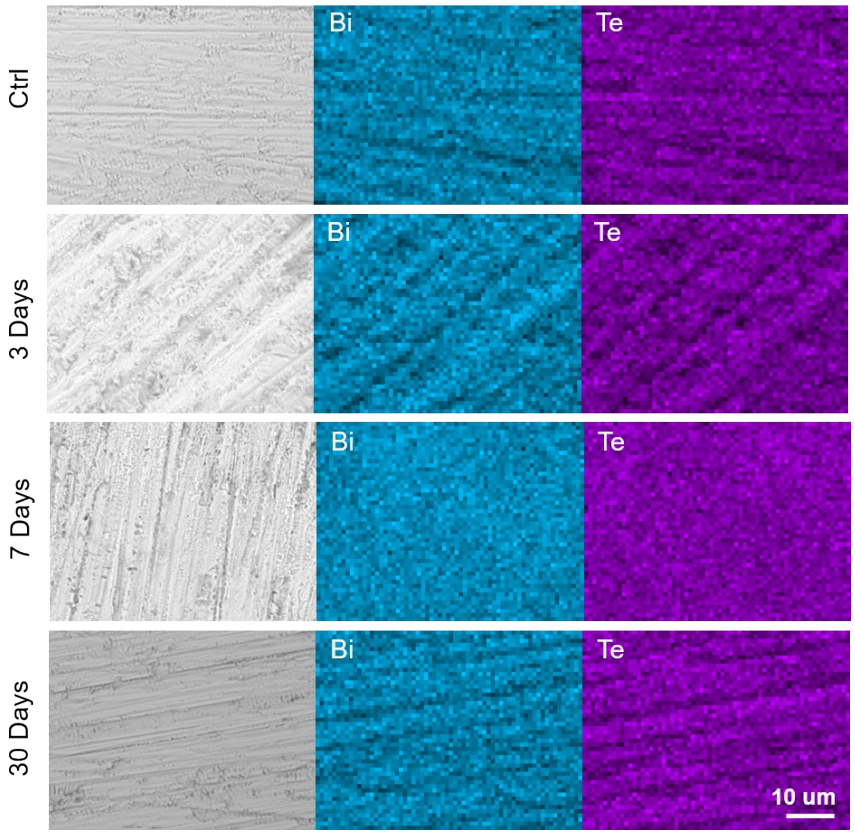

Fig. S13. SEM images and corresponding EDS mappings for Bi_2Te_3 after subcutaneous implantation for 3, 7, and 30 days.